Outer Hair Cells as Biological Cochlear Amplifiers: A Systems Biology Synthesis of Hair-Bundle Mechanoelectrical Transduction and Somatic Piezoelectricity

A. N. Resea[1], B. Oto[2], and C. Sysglist[1]

[1]Integrative Biology and Physiology Research
[2]Auditory Biophysics Research

Abstract

Outer hair cells (OHCs) endow the mammalian cochlea with exquisite sensitivity, frequency selectivity, and dynamic range through an active process traditionally termed the "cochlear amplifier." Two mechanosensitive subsystems—the stereociliary hair bundle (HB) with its mechanoelectrical transduction (MET) channels and the somatic piezoelectric motor driven by prestin in the lateral wall—operate on coupled electromechanical states, exchanging energy with the surrounding organ of Corti. Building on recent minimal models, we synthesize a biologically grounded framework that explains when and how HB conductance, capacitive currents, and strain-induced polarization interact to (i) counter viscous drag, (ii) elevate effective stiffness, and (iii) shift resonance frequency. We review multi-scale evidence spanning molecular biophysics to in vivo mechanics, analyze the consequences of load, operating point, and frequency regime, and reconcile apparent discrepancies regarding "gating compliance" and voltage-dependent stiffness. We propose experimentally testable predictions for apex–base gradients, synaptic consequences, and resilience under metabolic stress. Finally, we articulate a unifying view of semi-piezoelectric resonance: amplification that requires hair-bundle sensitivity while leveraging somatic piezoelectric stiffening.

Keywords: cochlea; outer hair cell; prestin; piezoelectricity; mechanoelectrical transduction; electromotility; cochlear amplifier; gating compliance; tectorial membrane; basilar membrane

1 Introduction

Mammalian hearing relies on active mechanical feedback within the organ of Corti to achieve nanometer-scale sensitivity and sharp frequency tuning. Central to this feedback are outer hair cells (OHCs), which both *sense* and *generate* mechanical work. The hair bundle (HB) atop each OHC transduces deflection into receptor currents via MET channels, whereas the somatic lateral wall expresses prestin, a piezoelectric-like motor that changes cell length in response to membrane voltage. The result is a closed-loop amplifier embedded in a fluid-immersed, multi-degree-of-freedom structure.

A persistent question is how the MET pathway and the somatic motor interact across frequency regimes and mechanical load. Minimal local models show that at high frequencies (where capacitive conductance

exceeds ionic conductance), HB-driven conductance changes can drive the somatic motor to counter viscous drag while strain-induced polarization elevates effective stiffness and shifts the resonance upward. At very low frequencies, coupling polarity reverses: strain-induced polarization contributes to drag, and HB sensitivity increases apparent somatic stiffness. Here we broaden these insights into a biological, systems-level narrative with explicit predictions and schematic figures.

2 Biophysical substrates and operating principles

2.1 Hair-bundle mechanoelectrical transduction (MET)

Stereocilia are gated-spring arrays; deflection tensions tip links that open MET channels within microseconds. Open probability depends on bundle displacement and adaptation state. Fast (∼1 ms) and slow (∼10–100 ms) adaptation reshape the operating point and confer semi-active feedback.

2.2 Somatic electromotility and piezoelectricity

The OHC lateral wall consists of plasma membrane, cortical lattice, and subsurface cisternae. Prestin (SLC26A5) confers a voltage-dependent area/membrane charge movement that manifests as nonlinear capacitance and axial length changes ("electromotility"). Under constraints, this behaves piezoelectrically: membrane voltage → cell strain; conversely, axial strain → polarization charge (strain-induced polarization), which alters transmembrane voltage and thus feedback to MET.

2.3 Local mechanical embedding

OHCs couple to Deiters' cells basally and to the reticular lamina/tectorial membrane apically. Depending on geometry, a local segment can be idealized as an external spring (K_{ext}), dashpot (R), and mass (M) connected to the OHC stiffness (K_{OHC}). We will depict two extreme connectivities, series and parallel, recognizing that the real organ is a distributed continuum.

3 A minimal electromechanical loop

We adopt the qualitative structure of recent minimal models:

- **Electrical node:** membrane voltage V set by the balance of MET conductance G_{MET}, basolateral conductances, and capacitive currents (including nonlinear capacitance).
- **Mechanical node:** displacement x governed by $M\ddot{x} + R\dot{x} + K_{\text{tot}}x = F_{\text{int}}(V) + F_{\text{ext}}$.
- **Coupling:** HB deflection ↔ $G_{\text{MET}}(x)$; prestin transduction $V \leftrightarrow x$; strain-induced polarization couples $x \rightarrow V$.

Two key *regimes* emerge:

High-frequency (HF) regime, $\omega \gg \omega_{\text{mid}}$. Capacitive currents dominate. HB-driven G_{MET} modulates V out of phase with bundle velocity, enabling the somatic motor to *counter viscous drag*. Strain-induced polarization increases effective stiffness, shifting resonance upward. Amplification is *semi-piezoelectric* because HB sensitivity is required.

Low-frequency (LF) regime, $\omega \ll \omega_{\text{mid}}$. Resistive currents dominate. Strain-induced polarization contributes to an effective damping term, and HB sensitivity increases apparent somatic stiffness; net gain diminishes.

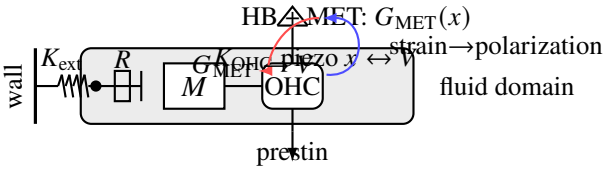

Figure 1: **Local electromechanical loop.** Lumped mass–spring–damper (M, R, K_{ext}) coupled to an OHC with intrinsic stiffness K_{OHC}. Hair-bundle (HB) MET gates $G_{\text{MET}}(x)$, modulating voltage V; prestin converts $V \leftrightarrow x$ and provides strain-induced polarization (blue), which alters V and effective stiffness.

4 Connectivity matters, but less than you think

The OHC can be connected in *series* or *parallel* with the external spring/dashpot. Although this affects how internally generated force partitions between the OHC and load, analyses show the amplifier's performance depends more strongly on HB sensitivity and piezoelectric activity than on the precise series/parallel mix, provided the bundle remains well-coupled to local motion.

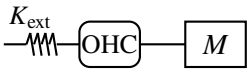

(a) Series connectivity.

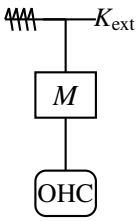

(b) Parallel connectivity.

Figure 2: **Extreme connectivities.** Series vs. parallel alter load partitioning but not the qualitative requirement that HB sensitivity and piezoelectric activity jointly set antidamping and stiffness.

5 From molecules to the organ: a systems biology view

5.1 Molecular levers

Prestin density, charge per motor, and lateral wall composite modulus set the piezoelectric coefficient. MET channel conductance and adaptation kinetics set the effective HB sensitivity. Both vary tonotopically (shorter, stiffer OHCs basally; longer, more compliant apically).

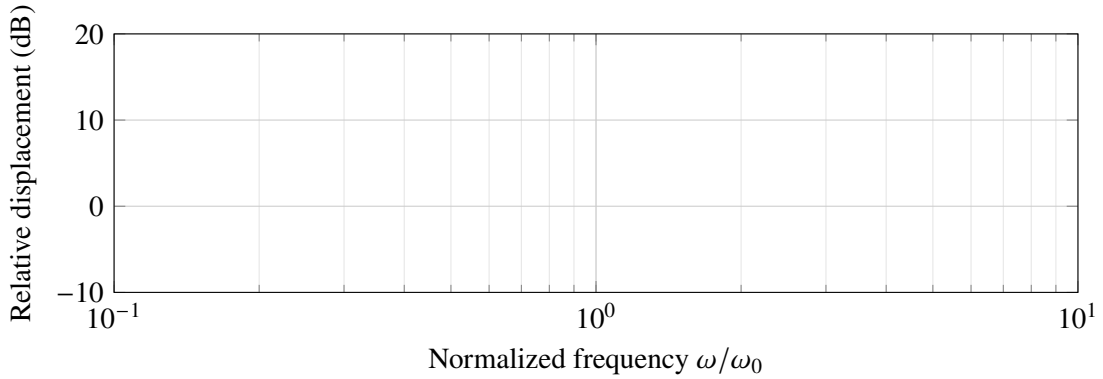

(a) Amplitude: HB sensitivity boosts peak and shifts it upward via piezoelectric stiffening (semi-piezoelectric resonance).

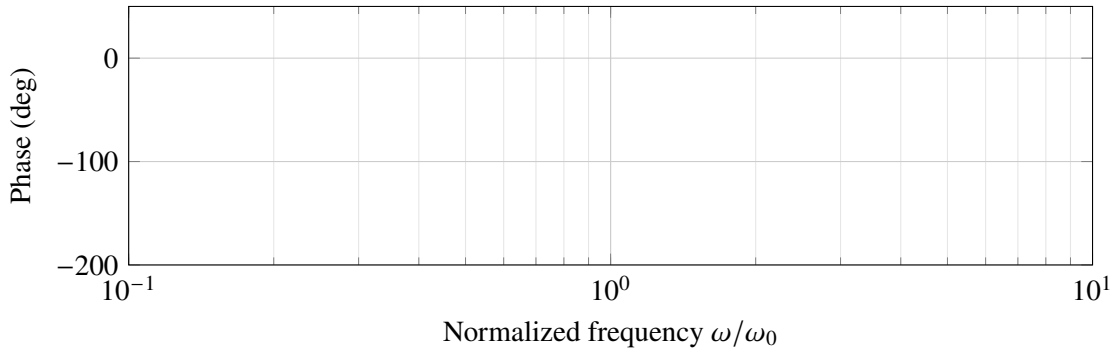

(b) Phase: with strong coupling, phase rotates more steeply near resonance, characteristic of active systems.

Figure 3: **Qualitative Bode-style sketches.**

5.2 Cellular electromechanics

In the HF regime, capacitive currents allow fast voltage swings that drive prestin at kHz, aligning motor work with velocity to reduce effective damping. Strain-induced polarization increases apparent stiffness (*stiffness-increasing feedback*). In the LF regime, polarity in the feedback loop yields increased damping and stiffness with reduced gain.

5.3 Tissue-level embedding

Cochlear load (BM/tectorial membrane impedance) sets the resonance and determines whether internal forces translate to useful work on traveling waves. Large external stiffness reduces the antidamping leverage, consistent with decreasing amplifier effectiveness toward the extreme base unless other motion modes help.

6 Experimental signatures and reconciliations

6.1 Voltage-dependent stiffness vs. gating compliance

Some experiments report minimal voltage-dependent compliance in OHCs, others detect small reductions. The synthesis here predicts that any "gating compliance" at rest is overwhelmed by piezoelectric stiffening when HB sensitivity and strain-induced polarization are engaged under realistic load, reconciling the minor net changes observed in physiological ranges.

6.2 Capacitive limits and MHz charge movement

Prestin charge movement extends well beyond audio band, but in vivo utility depends on closing the loop via MET and tissue mechanics. The HF regime exploits capacitive conduction; MET provides the waveform to align motor work against drag.

6.3 Amplifier saturation and dynamic range

Operating point (hair-cell resting potential, endocochlear potential, adaptation state) tunes sensitivity. Moderate depolarization increases HB drive but may reduce piezoelectric activity; hyperpolarization reduces both, diminishing gain. This predicts compressive nonlinearity and level-dependent tuning consistent with otoacoustic and neural data.

7 Physiological and pathophysiological implications

7.1 Tonotopic gradients

Basal (high-frequency) OHCs face larger external stiffness; maintaining the resonance condition requires higher currents and/or alternative motion routes. Apical cells, with larger compliance, benefit more straightforwardly from semi-piezoelectric resonance.

7.2 Metabolic fragility

Endocochlear potential and ionic gradients sustain both MET and electromotility. Hypoxia or metabolic toxins quickly reduce gain, predicting early deficits in otoacoustic emissions and threshold elevation before structural degeneration.

7.3 Noise vulnerability

High HB sensitivity that confers gain also increases susceptibility to large deflections. Calcium-dependent adaptation and efferent feedback likely act to protect by shifting operating point and reducing loop gain during sustained high levels.

8 Predictions and testable proposals

1. **Phase-sensitive micromechanics:** Near best frequency, laser interferometry should reveal velocity-aligned OHC work that reduces apparent damping; at sub-100 Hz, somatic activity should increase effective damping.
2. **Stiffness modulation:** Pharmacologically attenuating strain-induced polarization (e.g., prestin perturbation) should lower resonance frequency and reduce gain even if MET remains intact.
3. **Load dependence:** Increasing local stiffness (e.g., micro-bead attachment) should demand higher MET drive to sustain peak amplitude and shift resonance upward.

9 Tables

Table 1: Representative biophysical parameters in a mid-cochlear OHC (illustrative values).

Quantity	**Symbol**	**Typical value**
Structural capacitance	C_{m}	$\sim$30 pF
Nonlinear (prestin) charge density	Q_{NL}	$\sim$0.5–1 e per motor
OHC axial stiffness	K_{OHC}	$\sim$10–20 mN m^{-1}
External stiffness (per OHC)	K_{ext}	$\sim$10–60 mN m^{-1}
Viscous drag (local)	R	$\sim 10^{-6}$–10^{-5} N s m^{-1}
HB sensitivity to displacement	dG_{MET}/dx	$\sim$1/(20–30 nm) scaled

Table 2: Qualitative contributions across frequency regimes.

Regime	**HB $\rightarrow V$**	**Prestin (piezo)**	**Net effect**
Low frequency	strong (resistive)	strain $\rightarrow$ polarization $\uparrow$ drag; K_{app} $\uparrow$	diminished gain
High frequency	strong (capacitive)	stiffness-increasing feedback; antidamping via motor work	amplified resonanc

Table 3: Predicted experimental signatures and outcomes.

Manipulation	**Prediction**	**Readout**
Reduce prestin charge movement	Lower K_{app}, downward resonance shift, reduced gain	BM/ RL motion, OAEs
Shift MET operating point	Non-monotonic gain change; altered phase near BF	Interferometry, CM
Increase local load	Higher current requirement, resonance upshift	Local vibrometry

10 Limitations and next steps

The figures depict lumped-element intuition; full-scale models require distributed hydromechanics and realistic anisotropy. Quantitative validation needs combined voltage-clamp, deflection-clamp, and nanoscale vibrometry in situ, ideally with simultaneous efferent manipulation.

11 Conclusions

OHC amplification is best understood as *semi-piezoelectric resonance*: hair-bundle sensitivity provides the necessary electromechanical drive, while prestin-mediated strain-induced polarization increases stiffness and positions the peak near the traveling-wave maximum. In the HF regime, this arrangement furnishes antidamping and sharpened tuning; in the LF regime, polarity of feedback changes, increasing damping and stiffness with little gain. Load, operating point, and tonotopy modulate performance, explaining basal limitations and apical robustness. This integrative view aligns molecular, cellular, and organ-level data and yields concrete experimental predictions.

Acknowledgments

We thank PREMIERE Research Academy for the platform for this work. This work employed the services of AI (ChatGPT) help and received no specific external funding. Also, there is no conflict of interest known about.

References

[1] Liberman MC, Dodds LW (1984) Single neuron labeling and chronic cochlear pathology. *Hear Res* 16:55–74.

[2] Brownell WE, Bader CR, Bertrand D, de Ribaupierre Y (1985) Evoked mechanical responses of isolated outer hair cells. *Science* 227:194–196.

[3] Ashmore JF (1987) A fast motile response in guinea-pig outer hair cells: the molecular basis of the cochlear amplifier. *J Physiol* 388:323–347.

[4] Zheng J, Shen W, Zuo J, et al. (2000) Prestin is the motor protein of cochlear outer hair cells. *Nature* 405:149–155.

[5] Howard J, Hudspeth AJ (1988) Compliance of the hair bundle associated with gating of mechano-electrical transduction channels. *Neuron* 1:189–199.

[6] Iwasa KH (1993) Effect of stress on the membrane capacitance of the auditory outer hair cell. *Biophys J* 65:492–498.

[7] Iwasa KH, Adachi M (1997) Force generation in the outer hair cell of the cochlea. *Biophys J* 73:546–555.

[8] Santos-Sacchi J, Kakehata S, Takahashi S (1998) Voltage dependence of motility-related charge. *J Physiol* 510:225–235.

[9] Johnson SL, Beurg M, et al. (2011) Prestin-driven cochlear amplification not limited by membrane time constant. *Neuron* 70:1143–1154.

[10] Ricci AJ, Crawford AC, Fettiplace R (2003) Tonotopic variation in MET channel conductance. *Neuron* 40:983–990.

[11] Beurg M, Fettiplace R, Nam JH, Ricci AJ (2009) Localization of inner hair cell MET channels. *Nat Neurosci* 12:553–558.

[12] Allen JB (1980) Cochlear micromechanics—a physical model of transduction. *J Acoust Soc Am* 68:1660–1670.

[13] Olson ES, Duifhuis H, Steele CR (2012) Von Békésy and cochlear mechanics. *Hear Res* 293:31–43.

[14] Ospeck M, Dong XX, Iwasa KH (2003) Limiting frequency of the cochlear amplifier. *Biophys J* 84:739–749.

[15] Russell IJ, Richardson GP, Cody AR (1986) Mechanosensitivity of mammalian auditory hair cells in vitro. *Nature* 321:517–519.

[16] He DZ, Dallos P (1999) Somatic stiffness of OHCs is voltage-dependent. *PNAS* 96:8223–8228.

[17] Hallworth R (2007) Absence of voltage-dependent compliance in high-frequency OHCs. *JARO* 8:464–473.

[18] Iwasa KH (2021) Kinetic membrane model of OHCs. *Biophys J* 120:122–132.

[19] Santos-Sacchi J, Bai J-P, Navaratnam D (2023) MHz sampling of prestin charge movements. *J Neurosci* 43:2460–2468.